Journal of Power Sources 224 (2013) 28–36

Contents lists available at SciVerse ScienceDirect

Journal of Power Sources

journal homepage: www.elsevier.com/locate/jpowsour

Enhanced proton conductivity of the proton exchange membranes by the phosphorylated silica submicrospheres

Yuning Zhao [a], Zhongyi Jiang [a], Daoshu Lin [b], Anjie Dong [b], Zhen Li [a], Hong Wu [a,c,*]

[a] *Key Laboratory for Green Chemical Technology, Ministry of Education of China, School of Chemical Engineering and Technology, Tianjin University, Tianjin 300072, China*
[b] *Department of Polymer Science and Technology, School of Chemical Engineering and Technology, Tianjin University, Tianjin 300072, China*
[c] *Tianjin Key Laboratory of Membrane Science and Desalination Technology, Tianjin University, Tianjin 300072, China*

HIGHLIGHTS

- ► Phosphorylated silica with different chain lengths and $-PO_3H_2$ amounts were prepared.
- ► SPEEK membranes doped with phosphorylated silica were fabricated.
- ► Proton conductivity was dependent on the $-PO_3H_2$ amounts and grafted chain lengths.
- ► The highest conductivity was 0.335 S cm^{-1} at 60 °C (100 RH).
- ► The proton conduction was tentatively explained by effective acidic group amounts.

GRAPHICAL ABSTRACT

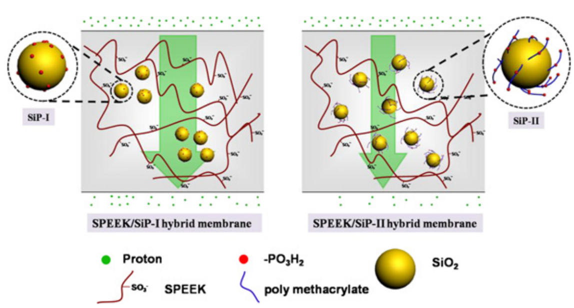

ARTICLE INFO

Article history:
Received 4 July 2012
Received in revised form
18 September 2012
Accepted 20 September 2012
Available online 29 September 2012

Keywords:
Phosphorylated silica submicrosphere
Sulfonated poly(ether ether ketone)
Hybrid membrane
Proton conductivity

ABSTRACT

Two kinds of phosphorylated silica submicrospheres were synthesized and incorporated into the sulfonated poly(ether ether ketone) (SPEEK) matrices to fabricate the hybrid membranes. Phosphorylation was carried out by the reaction of phosphorus oxychloride and the epoxy groups on the silica surface introduced by glycidyl-silane (SiP-I) or poly(glycidyl methacrylate) (SiP-II). The length of the chains and the amount of phosphoric acid groups ($-PO_3H_2$) grafted on the silica surface were tuned by the above two different phosphorylation methods. The dispersion of SiP-II, anti-swelling and methanol resistant property of the SPEEK/SiP-II hybrid membranes were all enhanced. And the proton conductivity was increased by doping with both kinds of phosphorylated silica particles. While the SPEEK/SiP-I hybrid membranes with less amounts of $-PO_3H_2$ groups showed unexpectedly much higher proton conductivities than the SPEEK/SiP-II hybrid ones at the same loadings ranging from 5 wt% to 20 wt%, and the highest reached 0.335 S cm^{-1} at 60 °C and 100% RH. The result was tentatively discussed in terms of effective proton-conducting groups/sites instead of the absolute amount of acidic groups.

1. Introduction

Proton exchange membrane fuel cells (PEMFCs) are potential candidates for applications in energy conversion and storage, and can be used in diverse fields, including portable, stationary and transportation uses [1]. Direct methanol fuel cells (DMFCs) are attractive for the use of liquid feed fuel which simplifies the fuel delivery and storage to some extent [2]. Extensive studies have been reported to

* Corresponding author. Key Laboratory for Green Chemical Technology, Ministry of Education of China, School of Chemical Engineering and Technology, Tianjin University, Tianjin 300072, China. Tel./fax: +86 022 23500086.
E-mail address: wuhong2000@gmail.com (H. Wu).

0378-7753/$ – see front matter © 2012 Elsevier B.V. All rights reserved.
http://dx.doi.org/10.1016/j.jpowsour.2012.09.080

develop organic–inorganic hybrid membranes for the enhancement of the fuel cell performance, attributed from the combination of the advantages of the inorganic fillers (*e.g.*, mechanical, thermal and chemical stability) and the organic polymer matrix (*e.g.*, flexibility, ductility and the ease of processability) [3].

Nowadays, sulfonic acid groups ($-SO_3H$) are most widely used as proton conducting sites which are sensitive to the humidity [4]. To render the PEMs with enhanced water retention property, a variety of hygroscopic solid or porous inorganic fillers have been incorporated into polymer matrix, which exhibited high concentration of hydroxyl or/and acidic groups and rich hydrogen-bonding sites [1,5]. Among them, silica is most widely used due to its hygroscopic nature, versatile functionality and rich amount in nature. To endow silica the proton conductive property, sulfonation was explored extensively because of the relatively high proton conductivity of the $-SO_3H$ groups at highly hydrated conditions and the liability of functionalization. Sulfonation could be achieved by the reaction with reagent like chlorosulfuric acid and the proton conductivity of the hybrid membranes could be compensated or improved after the introduction of the proton-conducting acidic sites [6].

Recently, much more attention has been directed toward PEMs based on phosphoric acid groups ($-PO_3H_2$) as alternatives for DMFC applications. Compared with $-SO_3H$ groups, the amphoteric and high dielectric constant property of the $-PO_3H_2$ groups can facilitate the self-dissociation and charge separation of the acid and thus leading to a high concentration of proton, which is especially beneficial for the membrane performance in the high temperature and low humidity environments [7,8]. The higher water binding energy (47.3 kJ mol^{-1} and 44.4 kJ mol^{-1} for $-PO_3H_2$ and $-SO_3H$, respectively) and the lower average zero point energy of $-PO_3H_2$ (37.2 kJ mol^{-1} and 69.9 kJ mol^{-1} for $-PO_3H_2$ and $-SO_3H$, respectively) imply the higher water retention property and lower proton conduction barrier [9]. $-PO_3H_2$ groups also display better thermo-oxidative stability [7]. Hence, PEMs such as phosphorylated polymeric or organic–inorganic hybrid membranes have triggered intensive research interest. Different from the vast kinds of sulfonated polymer materials, the direct polymerization of the phosphorylated monomers or the post-phosphorylation of the polymer main chains were studied sparsely due to the more complicated chemistry and synthetic procedures [10]. Facile phosphorylation methods were developed by doping phosphoric acid (H_3PO_4) into the polymer matrix, mainly polybenzimidazole (PBI) [11]. While H_3PO_4 was soluble in water and could leach out under the humid fuel cell application environments, thereby phosphorylated hybrid membranes made by fixing $-PO_3H_2$ groups on inorganic supports, like silica materials, were competitive candidates. The phosphorylated silica materials could be synthesized via co-condensation of hydrolyzed phosphoric-silane and tetraethyl orthosilicate (TEOS) [12,13]. When utilized in the intermediate-temperature and low-humidity PEMFCs, the inherent water retention capacity, high thermal stability and the contribution to the proton conductivity of the phosphorylated silica materials, were advantageous for the improvement of the membrane performance. The proton conductivity at 85 °C and 50% RH of the hybrid membrane doped with phosphorylated silica was reported to be 0.026 S cm^{-1}, which was 24% higher than that of the pristine Nafion® membrane. It was accepted that small condensed units, such as oligomers, were preferentially yielded with the sol–gel reactions of the trifunctional organoalkoxysilanes (phosphoric-silanes) [14], thus silica materials could be synthesized first and phosphorylated consequently. Because the Si-OH groups were relatively inert to the phosphorylation reactions, the surface of silica were usually modified first, *e.g.*, by titanium isopropoxide, and then phosphorylated [15]. The phosphorylation degree was restricted by the direct modification methods mentioned above, since only a monolayer of the functional groups could be formed on the particle surface. Such a limitation could be alleviated by introducing phosphorylated polymer chains with more $-PO_3H_2$ groups. Diisopropyl *p*-vinylbenzyl phosphonate (DIPVBP) was emulsion-polymerized on the surface of silica spheres, and it was beneficial for the enhancement of the proton conductivity of the hybrid membranes (0.16 S cm^{-1} at 125 °C and 100% RH, while the proton conductivity of the recast Nafion® membrane decreased severely with the temperature exceeding 100 °C) [16,17]. The hygroscopic silica materials functionalized with phosphoric acid groups are promising for PEMs.

In this study, phosphorylated silica submicrospheres were incorporated into the sulfonated poly(ether ether ketone) membrane matrix to construct proton exchange membrane containing $-PO_3H_2$ groups. The silica submicrospheres were synthesized first to provide robust regular structure and then the phosphorylation was carried out on the silica surface to inhibit acid leaching and ensure stable acid immobilization. To realize facile phosphorylation, the silica surface was activated first by epoxy groups. The amounts of $-PO_3H_2$ groups were controlled by changing the modification methods. Meanwhile the existence form of the acid groups was altered by varying the chain lengths immobilized on the silica surface. The influences of the amounts of acidic groups and the chain lengths on the performance of the hybrid membranes, including proton conductivity, methanol permeability and the dispersions of fillers were explored.

2. Experiment

2.1. Materials and chemicals

TEOS (reagent grade), 3-glycidyloxypropyltrimethoxysilane (GPTMS, analytical reagent (AR)), 3-aminopropyltriethoxysilane (APTES, AR), glycidyl methacrylate (GMA, AR), phosphorus oxychloride ($POCl_3$, >98 wt%) and polyether ether ketone (PEEK 381G) were purchased from Sigma–Aldrich Co. LLC., Aladdin-reagent, J&K Scientific Ltd. (Beijing), Aladdin-reagent, Shanghai Guangzan Chemical Scientific Ltd. and Victrex England, respectively, and used without further purification. Toluene (AR) was purchased from Tianjin Jiangtian Chemical Technology Co., Ltd. and was distilled prior to use. Triethylamine, 2-bromoisobutyryl bromide, CuBr and N,N,N′,N″,N″-pentamethyldiethylenetriamine (PMDETA) were purchased from Sigma–Aldrich Co. LLC. and used without further purification (reagent grade).

All the other materials and chemicals were commercially available with analytical pure degree, and used as received. Deionized water was used throughout the work.

2.2. Preparation of the phosphorylated glycidyl-silane modified silica submicrospheres (SiP-I)

2.2.1. Preparation of silica submicrospheres (SiO_2)

Silica submicrospheres (SiO_2) were prepared by the Stöber method [18]: TEOS (10 mL) was added dropwise to the well-mixed solution of ethanol (200 mL), water (20 mL), and ammonia solution (6 mL) under vigorous stirring and the solution was kept stirring at room temperature overnight. The SiO_2 were purified by three cycles of centrifugation and re-suspended in ethanol with ultrasonic-bathing (ethanol washing), and dried in a vacuum oven at room temperature till constant weight.

2.2.2. Preparation of submicrospheres modified by glycidyl-silane (SiO_2-epoxy)

2 mL GPTMS was used to react with 2 g dry SiO_2. To avoid the silane coupling agents from hydrolyzing before reacting, SiO_2 was dispersed in 120 mL anhydrous toluene and then the mixture was

refluxed for 24 h. The SiO_2-epoxy were purified by three cycles of centrifugation and re-suspended in water and ethanol with ultrasonic-bathing (water and ethanol washing) and dried under vacuum freeze-drying.

2.2.3. Phosphorylation of silicas

To carry out the phosphorylation of silicas, excess $POCl_3$ was used to react with the epoxy group of SiO_2-epoxy [19,20]. In a typical way, 2 g SiO_2-epoxy was dispersed in 120 mL $POCl_3$ and the mixture was kept at 80 °C under vigorous stirring for 24 h. The final products were purified by more than three cycles of centrifugation, water washing and dried under vacuum freeze-drying. The phosphorylated spheres were denoted as SiP-I, where I referred to the phosphorylated SiO_2-epoxy.

2.3. Preparation of the phosphorylated poly(glycidyl methacrylate) grafted silica submicrospheres (SiP-II)

2.3.1. Preparation of submicrospheres modified by amino-silane (SiO_2—NH_2)

SiO_2 prepared by the Stöber method was modified by amino-silane in the same way with SiO_2-epoxy, except the replacement of GPTMS by APTES, and the modified SiO_2 was denoted as SiO_2—NH_2.

2.3.2. Surface initiated atom transfer radical polymerization (SI-ATRP) of GMA onto the surface of SiO_2—NH_2

Before the ATRP polymerization, ATRP functionalities were anchored onto the surface of SiO_2—NH_2: 2 g SiO_2—NH_2 was dispersed in 120 mL dry toluene containing 2% (V/V) triethylamine, followed by adding 2 mL ATRP initiator 2-bromoisobutyryl bromide dropwise into the solvent. The mixture was first kept in ice-water bath for 1 h and then at room temperature for another 24 h. The ATRP functionalities coated silicas (SiO_2—Br) were purified by more than three cycles of centrifugation, ethanol and acetone washing, and dried under vacuum freeze-drying.

ATRP polymerization was carried out as follows: 1 g ATRP tetrainitiator SiO_2—Br was dispersed in 60 mL anhydrous toluene in Sclenck flask, then 0.049 g CuBr, 0.144 mL degassed PMDETA and 2 mL GMA were added to the flask. The mixture was degassed by three freeze—pump—thaw cycles under Ar atmosphere. The reaction was performed for 14 h at 60 °C with vigorous stirring. The GMA polymerized silicas (SiO_2-PGMA) were purified by more than three cycles of centrifugation, tetrahydrofuran and ethanol washing and dried under vacuum freeze-drying.

2.3.3. Phosphorylation of silicas

The phosphorylation was carried out the same with the phosphorylation of SiO_2-epoxy, except the replacement of SiO_2-epoxy by SiO_2-PGMA, and the phosphorylated spheres were denoted as SiP-II, where II referred to the phosphorylated SiO_2-PGMA.

^{13}C NMR for SiP-II: δ 18.2 (CH_3), 31.4 ($CH_2C(CH_3)$), 41.7 ($CH_2C(CH_3)$), 67.5 ($C(O)OCH_2CH$), 59.7 ($CHCH_2O$), 179.3 ($CC(O)OCH_2$) [20–23].

2.4. Sulfonation of PEEK

Sulfonated poly(ether ether ketone) (SPEEK) was prepared via post-sulfonation according to the procedure in the literature [24]. In a typical way, 28 g dry PEEK (previously dried at 80 °C for more than 24 h) was dissolved in 200 mL sulfuric acid at room temperature under vigorous stirring. After the dissolution, the temperature was elevated to 45 °C and kept stirring for 12 h. Then the dark red solution was decanting into a large excess of cold water. The crude product was washed with water until pH 7 and then dried in vacuum oven at room temperature till constant weight. The sulfonation degree (DS) of SPEEK was determined to be 66.0% through the titration method described in the Section 2.6.

2.5. Membrane preparation

Phosphorylated or non-phosphorylated silica submicrospheres were well dispersed in the homogeneous DMF solutions of SPEEK (the content of SPEEK was 10 wt%). Then the membranes were prepared by casting the solution on a clean glass plate, followed by drying first at 60 °C for 12 h and then at 80 °C for another 12 h. The pristine SPEEK membrane was made in the same method. The as-prepared hybrid membranes containing SiP-I (or SiP-II, SiO_2) were denoted as SPEEK/SiP-I-Z% (or SPEEK/SiP-II-Z%, SPEEK/SiO_2-*Z* %), where *Z* referred to the weight percentage of SiP-I (or SiP-II, SiO_2) relative to the SPEEK matrix.

2.6. Characterizations

The size and morphology of the submicrospheres were characterized by transmission electron microscopy (TEM, JEOL, Tecnai G2 20 S-TWIN). ^{13}C solid state NMR spectrum was recorded on a 75 MHz Varian InfinityPlus 300 spectrometer in a magic angle spinning (MAS) probe (75.40004 MHz) using the pulse-mode CP-MAS (Chemagnetic 7.5 mm) method.

The phosphorus content in the submicrospheres was measured by Inductively Coupled Plasma Optical Emission Spectrophotometer (ICP, ICP-9000(N + M), USA Thermo Jarrell-Ash Corp.). The surface elemental composition of the phosphorylated submicrospheres was characterized by X-ray photoelectron spectroscopy (XPS) with a PHI 1600 spectrometer and Mg Kα radiation for excitation.

The cross-sectional morphology of the membranes was observed using field emission scanning electron microscope (FESEM, Nanosem 430) operated at 10 keV.

Thermogravimetric analyses (TGA, TA-50, Shimadzu, Japan) of both the submicrospheres and the membranes were recorded from the room temperature to 800 °C at a heating rate of 10 °C min^{-1} in nitrogen atmosphere (the flow rate of 30 mL min^{-1}). Differential scanning calorimetry (DSC) measurements were carried out on a DSC 204 F1 NETZSCH instrument with a heating or cooling rate of 10 °C min^{-1} in N_2 flow to determine the glass transition temperature (T_g) of the membranes [25,26].

2.7. Water uptake, swelling, sulfonation degree and ion-exchange capacity

The water uptake and the swelling can be derived from the weight and area of the membrane gained after fully hydration, respectively, in accordance with the previous work [27]. The measurements were repeated three times, and the error was within ±5%. Then the water uptake and swelling were calculated according to the following equations (Eqs. (1) and (2)), respectively.

$$\text{Water uptake}(\%) = \frac{W_{wet} - W_{dry}}{W_{dry}} \times 100 \quad (1)$$

$$\text{Swelling}(\%) = \frac{A_{wet} - A_{dry}}{A_{dry}} \times 100 \quad (2)$$

where W_{dry} and A_{dry} were the weight (g) and area (cm^2) of the dry membranes, W_{wet} and A_{wet} were the weight (g) and area (cm^2) of the fully hydrated membranes, respectively.

The sulfonation degree (DS) of SPEEK was determined by titration method as described in the previous work [28]. After titration, the ion exchange capacity (IEC, mmol g^{-1}) value was calculated by Eq. (3).

$$\mathrm{IEC} = \frac{V_{\mathrm{NaOH}} \times C_{\mathrm{NaOH}}}{m} \tag{3}$$

where m was the weight (g) of the dry SPEEK in H^+ form, V_{NaOH} and C_{NaOH} were the volume (mL) and concentration (mol L^{-1}) of the NaOH solution, respectively.

DS was calculated according to Eq. (4):

$$\mathrm{DS\%} = \frac{M_{r\mathrm{SPEEK}}}{\frac{1000}{\mathrm{IEC}} - M_{r-\mathrm{SO_3H}}} \times 100 \tag{4}$$

where $M_{r\mathrm{SPEEK}}$ and $M_{r-\mathrm{SO3H}}$ were the molecular weight of the SPEEK monomer repeat unit (288) and $-SO_3H$ (80), respectively.

2.8. Methanol permeability

Methanol permeability (P, $cm^2\ s^{-1}$, 2 M methanol solution) was measured using a glass diffusion cell as described in the previous work [29], and was calculated from Eq. (5):

$$P = S\frac{Vl}{AC_{A0}} \tag{5}$$

where S was the slope of the straight line of methanol concentration in the compartment B versus time (mol $L^{-1}\ s^{-1}$); V was the volume of the compartment B (L); l and A were the thickness and the effective area of the membrane, respectively (cm, cm^2); C_0 was the initial methanol concentration in compartment A (mol L^{-1}).

2.9. Proton conductivity

A two-point-probe conductivity cell was used to determine the in-plane proton conductivity of the membranes as described in the previous work [27]. The relative humidity was kept at 100% and the testing temperature was controlled by the water vapor from the room temperature to 100 °C. The proton conductivity σ (S cm^{-1}) was calculated according to the following equation:

$$\sigma = \frac{l}{AR} \tag{6}$$

where l was the distance between the two electrodes (cm); A was the effective cross-sectional area of the membrane sample (cm^2); R was the measured membrane resistance (Ω).

3. Results and discussion

3.1. Characterizations of submicrospheres

The phosphorylation of silica submicrospheres was achieved by the reaction of $POCl_3$ with epoxy groups. By changing the introducing methods of epoxy groups on the silica surface, the immobilized chain lengths and the amounts of $-PO_3H_2$ groups were controlled. The morphology of the as-synthesized submicrospheres was demonstrated by TEM as shown in Fig. 1. Spherical silica particles with a uniform size of about 80 nm in radius (Fig. 1(a)) were produced by the Stöber procedure. After phosphorylation, the morphology and size of the silica (SiP-I and SiP-II) were unaltered.

The detailed chemical structure of the poly(glycidyl methacrylate), grafted from the surface of silica submicrospheres (SiP-II) by ATRP, was confirmed by ^{13}C solid state NMR spectrum (Fig. 2). The chemical shifts at 31.4, 41.7 and 59.7 ppm were assigned to $CH_2C(CH_3)$, $CH_2C(CH_3)$ and $CHCH_2O$ carbons, respectively. The methyl carbon from the methacrylic units was observed at 18.2 ppm. The peak at 179.3 ppm was assigned to the carbonyl

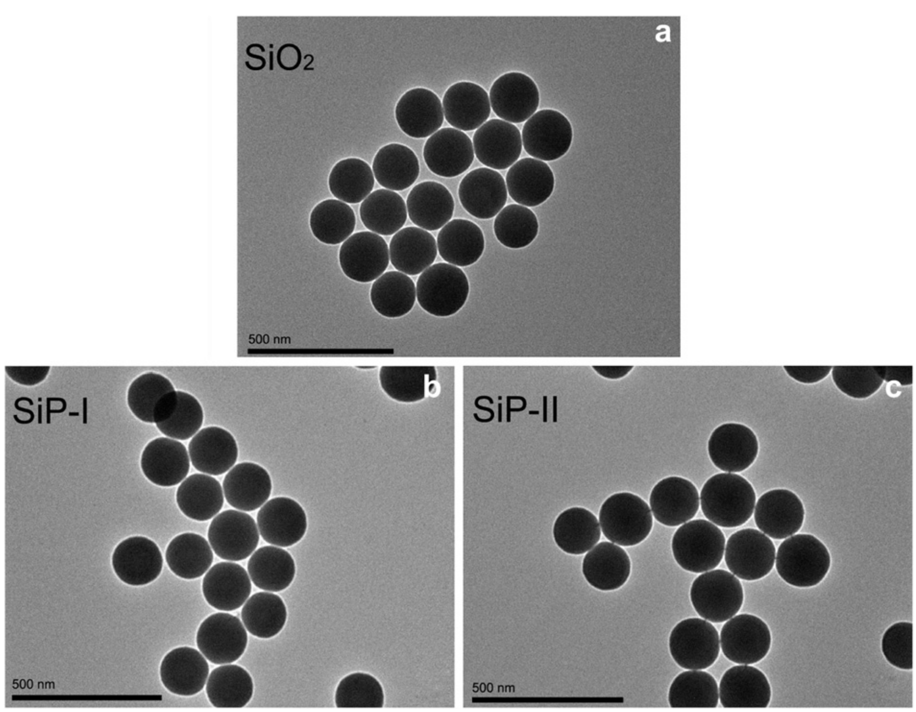

Fig. 1. TEM images of the (a) SiO_2, (b) SiP-I and (c) SiP-II submicrospheres.

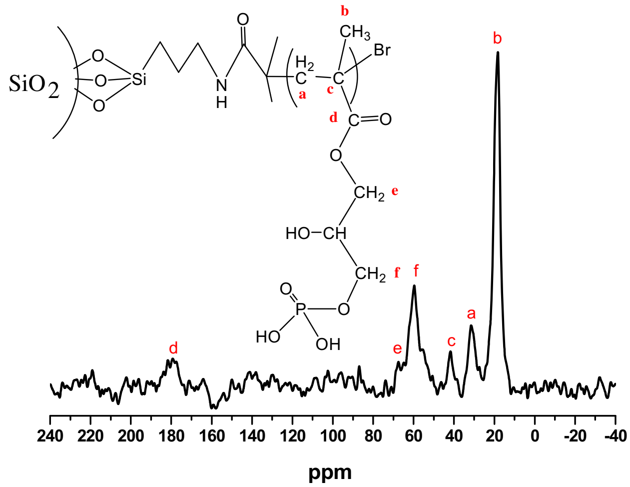

Fig. 2. Solid state ^{13}C NMR spectrum of the SiP-II submicrospheres.

carbons, and the signal at 67.5 ppm indicated the glyceryl spacer. Thus the proposed chemical structure of the grafted poly(glycidyl methacrylate) from the surface of SiP-II was confirmed. ICP was carried out to determine the content of phosphorus element (P) of both SiP-I and SiP-II, and the results were 1.54 wt% and 2.65 wt%, respectively. The weight percent of P element of SiP-II was higher than that of SiP-I by 72.0%, suggesting a higher amount of $-PO_3H_2$ groups on SiP-II. Hereby, the glycidyl methacrylate polymers on the surface of SiP-II exceeded the limitation of the monolayer of glycidyl-silane groups on the surface of SiP-I. The oxidation state of P element of SiP-I and SiP-II was analyzed by XPS spectrum, and the peak of binding energy at around 134.5 eV indicated the pentavalent-oxidation state of P (P^{5+}) and the presence of P–O bond [9]. According to the above characterizations, the schematic depictions of the possible chemical structure of the two kinds of phosphorylated silicas (SiP-I and SiP-II) were illustrated in Fig. 3.

3.2. Characterization of the hybrid membranes

The dispersion of the silica submicrospheres in the hybrid membranes was observed by SEM measurements (Fig. 4). It could be seen that with the 5 wt% loading (Fig. 4(b), (d) and (f) for the SPEEK/SiO_2, SPEEK/SiP-I and SPEEK/SiP-II membranes, respectively), the particles were homogeneously dispersed in all the membranes. When the loading increased to 15 wt%, aggregation occurred for both the SPEEK/SiO_2 (Fig. 4(c)) and SPEEK/SiP-I (Fig. 4(e)) membranes, while no obvious aggregation was observed for SPEEK/SiP-II (Fig. 4(g)) at the identical loading amount. Even with the loading as high as 40 wt% (Fig. 4(h)), SiP-II were still homogeneously dispersed.

The glass transition temperatures (T_gs) of the pristine and hybrid membranes determined by DSC were given in Table 1. A single glass transition temperature (T_g) was observed for SPEEK polymers at 226 °C which was consistent with that reported in literatures [25,30,31]. T_gs were decreased after the incorporation of both kinds of the phosphorylated silica submicrospheres, indicating that the SPEEK polymer chain matrix was disturbed and both the mobility and flexibility were enhanced by the introduction of inorganic particles. The $-PO_3H_2$ groups on the surface of phosphorylated silica submicrospheres exhibited electrostatic repulsion with the $-SO_3H$ groups in the polymer matrix, the SPEEK polymer chain packing between the inorganic–organic interface was disturbed and thus the local chain motions were enhanced [26,32]. After the introduction of the polymers grafted from SiP-II, the phosphorylation degree was promoted and the T_gs were further decreased for the increased electrostatic repulsion. A new T_g appeared at about 150 °C for all the SPEEK/SiP-II membranes, indicating a phase separation between the SPEEK matrix and the polymer chains grafted from the surface of SiP-II. This phase separation could be explained by the fact that the grafted carbon chains were more flexible compared to the rigid SPEEK chains with aromatic rings [30,33,34]. And the phase separation structure might impede the grafted polymer chains of SiP-II from further penetrating into the SPEEK matrix and might reduce the possible contribution of the $-PO_3H_2$ groups to the membrane proton conduction.

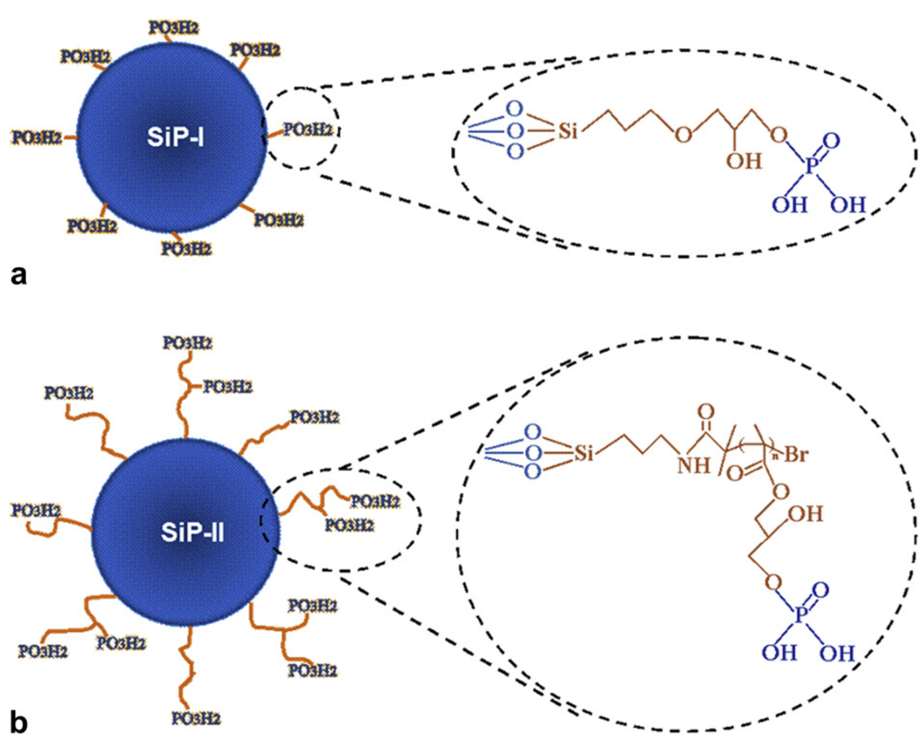

Fig. 3. The schematic depictions of the chemical structure of the phosphorylated silica submicrospheres.

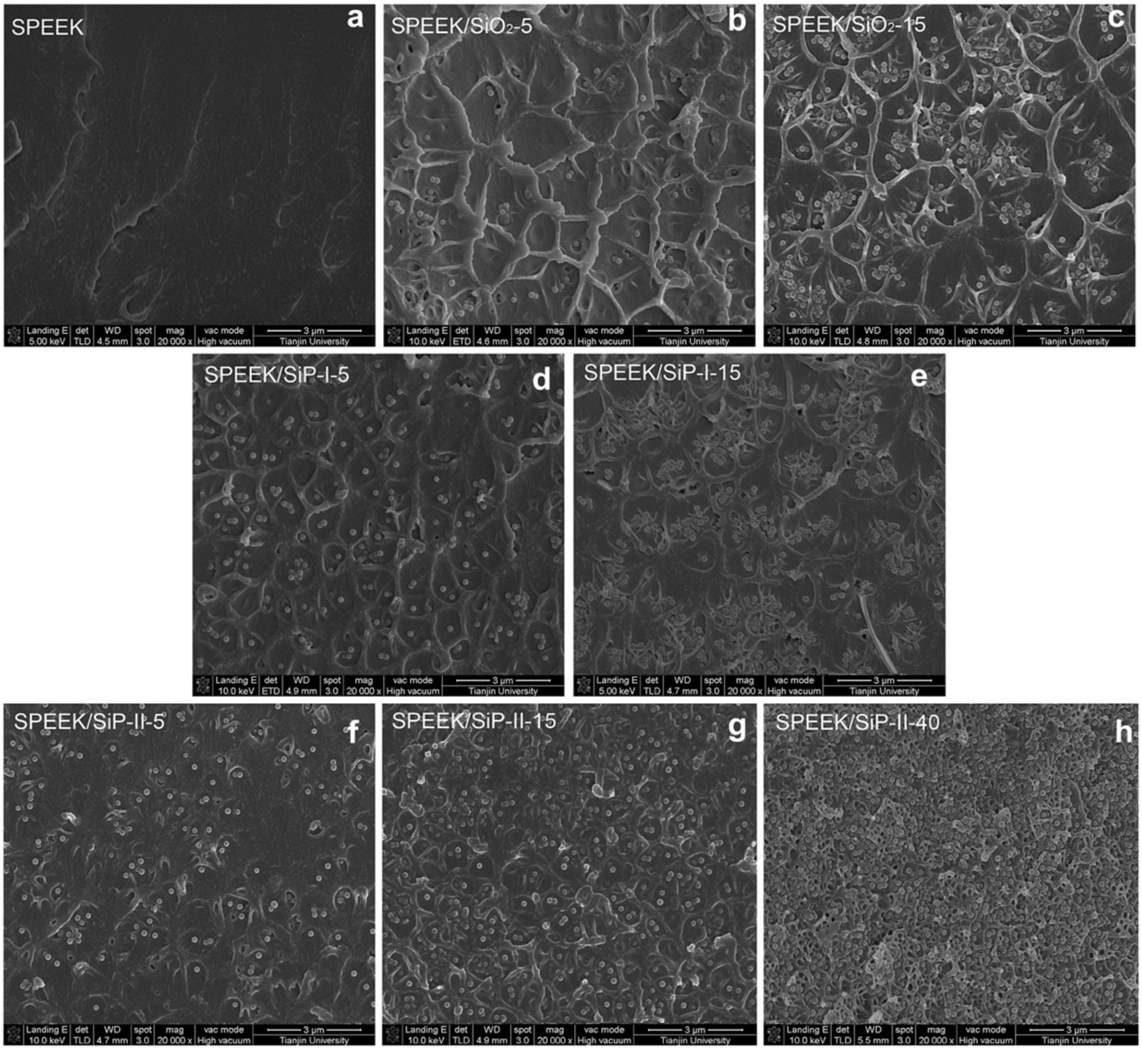

Fig. 4. FESEM images of the cross-section of the pristine SPEEK membrane and the SPEEK hybrid membranes: (a) SPEEK, (b) SPEEK/SiO_2-5, (c) SPEEK/SiO_2-15, (d) SPEEK/SiP-I-5, (e) SPEEK/SiP-I-15, (f) SPEEK/SiP-II-5, (g) SPEEK/SiP-II-15, (h) SPEEK/SiP-II-40. (The scales in all the images were 3 μm)

TGA was employed to study the thermal stability of the pristine SPEEK membrane and the hybrid membranes (Fig. 5). All the hybrid membranes showed quite similar decomposition patterns. Membrane samples had a typical three-steps degradation behavior, and the weight loss below about 110 °C was caused by the loss of moisture in the membrane [27,30]. The starting temperature of the first (T_{d1}), second (T_{d2}) and the last (T_{d3}) thermal degradation of SPEEK was around 235 °C, 323 °C and 522 °C, respectively. The weight loss between 235 °C and 323 °C was mainly associated with the loss of the $-SO_3H$ groups in the range of 250–280 °C, and the weight loss above 323 °C was related to the decomposition of the main chain of PEEK in the range of 400–580 °C [31]. It could be observed from TGA results that the thermal degradation temperatures of the hybrid membranes were almost unchanged, in other words, the addition of silica submicrospheres (SiP-I and SiP-II) into the polymer matrix did not significantly alter the thermal degradation mechanism of the hybrid membranes. Since the inorganic part of silica submicrospheres could act as superior insulator and transport barrier to the volatile products generated during the decomposition [35], the weight loss of the hybrid membranes was lower than the pristine SPEEK membrane, especially above T_{d2}. The total weight loss decreased with the increasing content of silica submicrospheres, and the SPEEK/SiP-I hybrid membranes possessed larger amount of inorganic parts than SPEEK/SiP-II membranes.

Table 1
Glass transition temperature (T_g) of the pristine SPEEK and SPEEK hybrid membranes.

Membrane	Transition temperature (°C)	
SPEEK	226	
SPEEK/SiP-I-5	219	
SPEEK/SiP-I-10	219	
SPEEK/SiP-I-15	216	
SPEEK/SiP-I-20	220	
SPEEK/SiP-I-30	222	
SPEEK/SiP-II-5	154	198
SPEEK/SiP-II-10	139	190
SPEEK/SiP-II-15	150	202
SPEEK/SiP-II-20	143	195
SPEEK/SiP-II-30	153	199
SPEEK/SiP-II-40	150	203

3.3. Water uptake, swelling property and methanol permeability of the hybrid membranes

Water plays an important role in the membranes, for the enhanced water uptake could hydrate the PEM membrane to

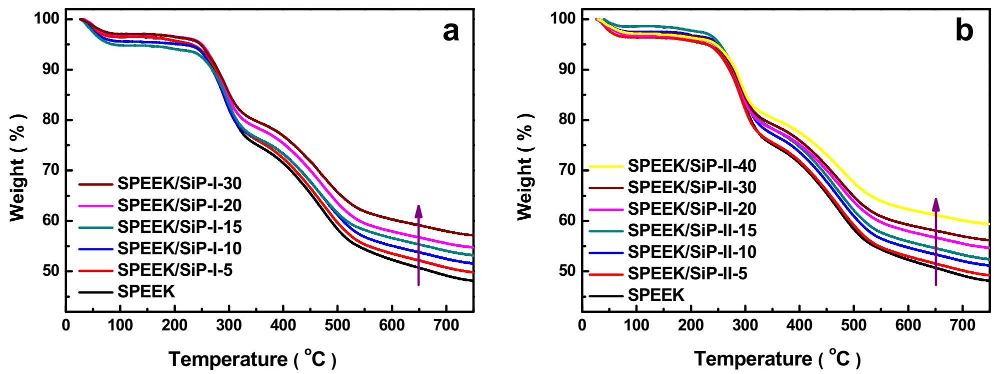

Fig. 5. TGA curves of the pristine SPEEK and SPEEK/SiP-I (a), SPEEK/SiP-II (b) hybrid membranes.

facilitate the proton conduction, while the excess swelling can result in the deterioration of the membrane–catalyst interface, severe water drag or fuel drag and possible performance failure of the fuel cell [3]. After the incorporation of the unmodified SiO_2, the water uptake and the swelling of the membranes increased and increased further with the content of SiO_2 (Fig. 6(a)), suggesting the existence of the defects in the SPEEK/SiO_2 membranes [36].

For the SPEEK/SiP-I membranes, the water uptake and the swelling were still higher than the pristine SPEEK membrane, but in a decreasing tendency. Hence, the existence of the defects in the membranes was also suggested, while the organic modified surface of SiP-I inhibited the further increase of the water uptake and swelling. The longer organic chain length of SiP-II endowed the particles with better dipersity with the polymer matrix than both SiO_2 and SiP-I (which could also be observed by SEM characterizations shown in Fig. 4). After the introduction of SiP-II, the water uptake and the swelling were decreased, and further decreased with the increasing content of the inorganic part. The highest reduction degree of swelling of SPEEK/SiP-II was 52.0% with 40 wt% of SiP-II.

The methanol permeability of the SPEEK/SiO_2 and SPEEK/SiP-I hybrid membranes were greater than the pristine SPEEK membrane (Fig. 6(b)), induced by the higher water uptake [37,38]. On the contrary, the methanol permeability of SPEEK/SiP-II membranes was reduced. The methanol permeability was in the same tendency with the water uptake properties.

3.4. Proton conductivity of the hybrid membranes

Proton conductivity of the membranes as a function of temperature at 100% RH was characterized by the aforementioned method and illustrated in Fig. 7. The proton conductivity of the pristine SPEEK membrane at 31.7 °C was 0.0548 S cm^{-1}, and increased with the rising temperature. After the incorporation of the unmodified SiO_2 submicrospheres, the proton conductivity was decreased and further decreased with the content of SiO_2 (Fig. 7(a)). On the contrary, proton conductivity was enhanced to different degrees with the introduction of SiP-I (Fig. 7(b)) and SiP-II (Fig. 7(c)). All the proton conductivities of the hybrid membranes were elevated with the increasing temperature. For the SPEEK/SiP-II membranes, the proton conductivity was enhanced with the content of SiP-II in the whole loading range. While the proton conductivities were elevated to higher degrees at the same doping level of inorganic particles for the SPEEK/SiP-I membranes, and the increase of the proton conductivity for SPEEK/SiP-I-30 membranes was reduced to nearly the same with SPEEK/SiP-I-5 membranes.

Two sorts of proton transport mechanisms were well accepted: the vehicle mechanism and the Grotthuss mechanism [27,39]. The former implied the diffusion of hydrated protons or proton-containing groups (*e.g.*, $H_5O_2^+$ ('Zundel' ion) and $H_9O_4^+$ ('Eigen' ion)) as a whole in a medium such as water; while the latter consisted of the diffusion of protonic defects, which were also called inherent protonic charge carriers or intrinsic proton conductivity, through the medium by continuous breaking and forming of hydrogen bonds [40]. To facilitate the fast proton conductivity through the membrane, not only the adequate proton-conducting sites were needed, but also abundant amount of effective proton-conducting groups was crucial. Compared to the SPEEK pristine membrane (IEC = 1.933 mmol g^{-1}) utilized in this work, the proton-conducting sites of Nafion® 117 membranes (IEC = 0.852 mmol g^{-1} [41]) were much less according to the IEC values. But the proton conductivity of Nafion® membrane was comparable or even better than the SPEEK pristine membrane (0.0696 S cm^{-1} [9] and 0.0548 S cm^{-1} for Nafion® and SPEEK, respectively. Both of them were determined in the same condition with the same equipment). The high proton conductivity of Nafion®

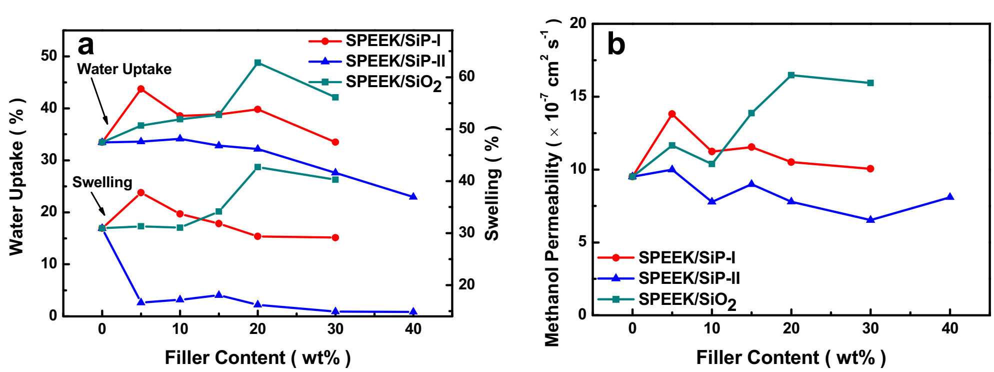

Fig. 6. The water uptake and swelling properties (a) and the methanol permeability (b) of the pristine SPEEK and SPEEK hybrid membranes at 25 °C.

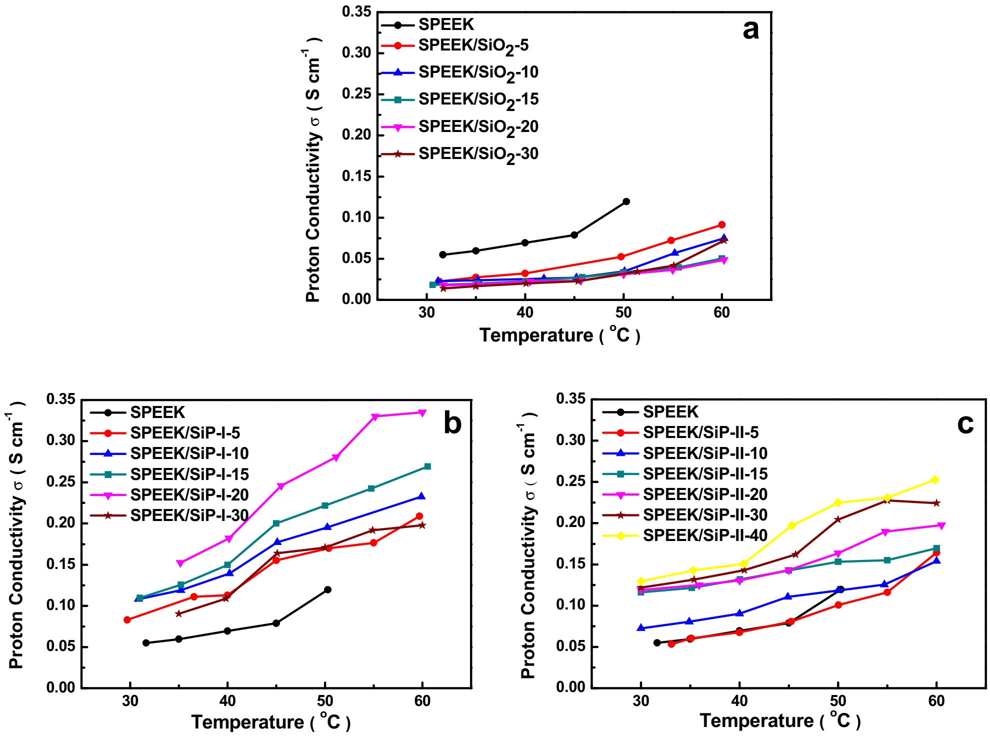

Fig. 7. Proton conductivity of the pristine SPEEK membrane and the SPEEK hybrid membranes as a function of temperature at 100% RH: (a) the SPEEK/SiO_2 hybrid membranes, (b) the SPEEK/SiP-I hybrid membranes, (c) the SPEEK/SiP-II hybrid membranes.

with much less proton-conducting sites could be attributed to the more separated, less branched, better interconnected and wider ionic channels in the membrane [42], thus producing higher amount of effective proton-conducting groups. In this work, both the amount of $-PO_3H_2$ groups and the length of the chain immobilized on the silica surface would affect the number of effective proton-conducting groups.

For the unmodified SiO_2 submicrospheres bore only weak acidic groups (silanols groups), SiO_2 acted as barrier for protons, leading to the decrease of the proton conductivity [43]. After the incorporation of the SiP-I and SiP-II, $-PO_3H_2$ groups were introduced into the membranes, and SiP-II bore more $-PO_3H_2$ groups and longer polymeric chains on the silica surface than SiP-I. However, phase separation of the polymer chains grafted on the surface of SiP-II and the SPEEK matrix was confirmed by the two distinct T_gs for all the SPEEK/SiP-II membranes as obtained from the DSC results. During the phosphorylation of epoxy groups, several side reactions could take place including the hydrolysis of the epoxy groups and the phosphates, and the crosslinking among the reactants [20]. Consequently, the grafted polymers were inhibited from penetrating into the SPEEK matrix, and the interactions between the acidic groups were reduced. Otherwise the intra- and intermolecular interactions between the $-PO_3H_2$ groups on SiP-I and the membrane matrix could be formed more easily and extensively than SiP-II. Therefore, the SiP-I even with less amounts of $-PO_3H_2$ groups exhibited more effective acidic groups for proton conducting. The proton conductivities of the SPEEK/SiP-I membranes were higher than the SPEEK/SiP-II membranes at the same doping level of inorganic particles and the highest conductivity of the SPEEK/SiP-I membranes was 0.335 S cm^{-1} at 60 °C (100 RH) with the content of 20 wt%. The reduction of the proton conductivity of the SPEEK/SiP-I membranes over the weight content of 20 wt% could be attributed to the large scale aggregation in the membrane (as observed in Fig. 4(d) and (e)), which leads to a sharp decrease of the amount of effective acidic groups. On the contrary, for the SPEEK/SiP-II membranes the proton conductivity still increased with the content of SiP-II in the whole loading range. The longer organic chain length of SiP-II rendered the particles better dispersity with the polymer matrix than both SiO_2 and SiP-I (confirmed by SEM characterizations shown in Fig. 4(f)–(h)), and no obvious aggregation occurred in all the SPEEK/SiP-II hybrid membranes from the loading content of 5 wt% to 40 wt%. With the increase of doping amount of SiP-II, more effective proton-conducting groups were introduced into the hybrid membranes, then contributing to the sustained increase of the proton conductivity.

Moreover, the mobility for both the water molecules and proton could be increased by the increase of the volume fraction of water, hence the higher water uptake of SPEEK/SiP-I membranes than SPEEK/SiP-II membranes also contributed to the better proton conductivity [16,40].

4. Conclusion

Phosphorylated silica submicrospheres were synthesized via phosphorylation of silane coupling agents modified (SiP-I) or polymer grafted (SiP-II) silica submicrospheres. The length of the grafted chains immobilized on the silica surface and the amounts of $-PO_3H_2$ groups can be controlled in a facile way and these two kinds of phosphorylated silica submicrospheres were incorporated into the SPEEK matrix to fabricate the SPEEK/SiP-I and SPEEK/SiP-II hybrid membranes. The SPEEK/SiP-II hybrid membranes containing polymer grafted phosphorylated silica submicrospheres were endowed with more phosphorylation sites, better homogeneity, lower swelling and higher methanol barrier properties, but the enhancement in the proton conductivities was less than that of the SPEEK/SiP-I hybrid membranes. The phase separation of the SPEEK matrix with the polymer chains grafted on the surface of SiP-II, as well as the crosslinking of the polymer chains might prevent the

full contact of the grafted polymer chains and the SPEEK matrix. Hence, the higher proton conductivities of the hybrid membranes doped with SiP-I (in the loading range except 30 wt% of SiP-I) could be tentatively attributed to the higher amounts of effective proton-conducting groups or sites. The highest conductivity in SPEEK/SiP-I hybrid membranes was 0.335 S cm^{-1} at 60 °C (100 RH) with 20 wt% of SiP-I. It was inspired that for the rational design of the hybrid membranes with enhanced proton conductivity, both the absolute/theoretical proton-conducting sites amount, and the effective/accessible proton-conducting sites amount should be taken into account for DMFC application.

Acknowledgments

The authors gratefully acknowledge financial support from Program for New Century Excellent Talents in University (NCET-10-0623), the Programme of Introducing Talents of Discipline to Universities (No. B06006), the Project-sponsored by SRF for ROCS, State Education Ministry and the National Science Fund for Distinguished Young Scholars (21125627).

References

[1] C. Laberty-Robert, K. Vallé, F. Pereira, C. Sanchez, Chem. Soc. Rev. 40 (2011) 961–1005.
[2] A.-C. Dupuis, Prog. Mater. Sci. 56 (2011) 289–327.
[3] B.P. Tripathi, V.K. Shahi, Prog. Polym. Sci. 36 (2011) 945–979.
[4] M.A. Hickner, H. Ghassemi, Y.S. Kim, B.R. Einsla, J.E. McGrath, Chem. Rev. 104 (2004) 4587–4612.
[5] C.H. Park, C.H. Lee, M.D. Guiver, Y.M. Lee, Prog. Polym. Sci. 36 (2011) 1443–1498.
[6] G. Gnana Kumar, A.R. Kim, K. Suk Nahm, R. Elizabeth, Int. J. Hydrogen Energy 34 (2009) 9788–9794.
[7] M. Schuster, T. Rager, A. Noda, K.D. Kreuer, J. Maier, Fuel Cells 5 (2005) 355–365.
[8] J. Lu, H. Tang, S. Lu, H. Wu, S.P. Jiang, J. Mater. Chem. 21 (2011) 6668–6676.
[9] J. Wang, Y. Zhao, W. Hou, J. Geng, L. Xiao, H. Wu, Z. Jiang, J. Power Sources 195 (2010) 1015–1023.
[10] A.L. Rusanov, P.V. Kostoglodov, M.J.M. Abadie, V.Y. Voytekunas, D.Y. Likhachev, Adv. Polym. Sci. 216 (2008) 125–155.
[11] C.-H. Shen, L.-c. Jheng, S.L.-c. Hsu, J. Tse-Wei Wang, J. Mater. Chem. 21 (2011) 15660–15665.
[12] K. Wang, S. McDermid, J. Li, N. Kremliakova, P. Kozak, C. Song, Y. Tang, J. Zhang, J. Zhang, J. Power Sources 184 (2008) 99–103.
[13] Y.G. Jin, S.Z. Qiao, Z.P. Xu, J.C.D. da Costa, G.Q. Lu, J. Phys. Chem. C 113 (2009) 3157–3163.
[14] Y.G. Jin, S.Z. Qiao, Z.P. Xu, Z. Yan, Y. Huang, J.C.D. da Costa, G.Q. Lu, J. Mater. Chem. 19 (2009) 2363–2372.
[15] J. Zhang, Z. Ma, J. Jiao, H. Yin, W. Yan, E.W. Hagaman, J. Yu, S. Dai, Langmuir 25 (2009) 12541–12549.
[16] L. Lou, H. Pu, Int. J. Hydrogen Energy 36 (2011) 3123–3130.
[17] H. Pu, H. Pan, Y. Qin, D. Wan, J. Yuan, Mater. Lett. 64 (2010) 1510–1512.
[18] W. Stöber, A. Fink, E. Bohn, J. Colloid Interface Sci. 26 (1968) 62–69.
[19] H. Egawa, T. Nonaka, J. Appl. Polym. Sci. 30 (1985) 3239–3247.
[20] R.O. Carter III, J.L. Parsons, J.W. Holubka, Ind. Eng. Chem. Res. 26 (1987) 1518–1523.
[21] X. Song, Y. Zhang, D. Yang, L. Yuan, J. Hu, G. Lu, X. Huang, J. Polym. Sci. A Polym. Chem. 49 (2011) 3328–3337.
[22] J. Yamanaka, T. Kayasuga, M. Ito, H. Yokoyama, T. Ishizone, Polym. Chem. 2 (2011) 1837–1848.
[23] M.M. Fares, S.M. Assaf, A.A. Jaber, J. Appl. Polym. Sci. 122 (2011) 840–848.
[24] H. Doğan, T.Y. Inan, E. Unveren, M. Kaya, Int. J. Hydrogen Energy 35 (2010) 7784–7795.
[25] B. Mecheri, A. D'Epifanio, L. Pisani, F. Chen, E. Traversa, F.C. Weise, S. Greenbaum, S. Licoccia, Fuel Cells 9 (2009) 372–380.
[26] J. Wang, X. Yue, Z. Zhang, Z. Yang, Y. Li, H. Zhang, X. Yang, H. Wu, Z. Jiang, Adv. Funct. Mater. (2012). http://dx.doi.org/10.1002/adfm.201201436.
[27] Y. Zhao, Z. Jiang, L. Xiao, T. Xu, H. Wu, J. Power Sources 196 (2011) 6015–6021.
[28] H. Wu, X. Shen, T. Xu, W. Hou, Z. Jiang, J. Power Sources 213 (2012) 83–92.
[29] Y. Zhao, Z. Jiang, L. Xiao, T. Xu, S. Qiao, H. Wu, Solid State Ionics 187 (2011) 33–38.
[30] M.N.A. Mohd Norddin, A.F. Ismail, D. Rana, T. Matsuura, S. Tabe, J. Membr. Sci. 328 (2009) 148–155.
[31] P. Xing, G.P. Robertson, M.D. Guiver, S.D. Mikhailenko, K. Wang, S. Kaliaguine, J. Membr. Sci. 229 (2004) 95–106.
[32] A.G. Kannan, N.R. Choudhury, N.K. Dutta, J. Membr. Sci. 333 (2009) 50–58.
[33] H.-Y. Jung, J.-K. Park, Electrochim. Acta 52 (2007) 7464–7468.
[34] D.J. Walsh, S. Rostami, Adv. Polym. Sci. 70 (1985) 119–169.
[35] H. Zou, S. Wu, J. Shen, Chem. Rev. 108 (2008) 3893–3957.
[36] J. Wang, X. Zheng, H. Wu, B. Zheng, Z. Jiang, X. Hao, B. Wang, J. Power Source 178 (2008) 9–19.
[37] A.F. Ismail, N.H. Othman, A. Mustafa, J. Membr. Sci. 329 (2009) 18–29.
[38] B. Baradie, J.P. Dodelet, D. Guay, J. Electroanal. Chem. 489 (2000) 101–105.
[39] L. Jiménez-García, A. Kaltbeitzel, V. Enkelmann, J.S. Gutmann, M. Klapper, K. Müllen, Adv. Funct. Mater. 21 (2011) 2216–2224.
[40] K.D. Kreuer, Solid State Ionics 136–137 (2000) 149–160.
[41] Z. Jiang, X. Zheng, H. Wu, J. Wang, Y. Wang, J. Power Sources 180 (2008) 143–153.
[42] K.D. Kreuer, J. Membr. Sci. 185 (2001) 29–39.
[43] Y. Jin, S. Qiao, J.C.D. da Costa, B.J. Wood, B.P. Ladewig, G.Q. Lu, Adv. Funct. Mater. 17 (2007) 3304–3311.